


RESEARCH ARTICLE

Widespread drought-induced leaf shedding and legacy effects on productivity in European deciduous forests

Adrià Descals^{1,2}, Aleixandre Verger^{1,3} , Gaofei Yin⁴, Iolanda Filella^{1,2} & Josep Peñuelas^{1,2}¹CREAF, Cerdanyola del Vallès, Barcelona 08193, Catalonia, Spain²CSIC, Global Ecology Unit CREAF-CSIC-UAB, Bellaterra, Barcelona 08193, Catalonia, Spain³CIDE, CSIC-UV-GV, València 46113, Spain⁴Faculty of Geosciences and Environmental Engineering, Southwest Jiaotong University, Chengdu 610031, China**Keywords**

Deciduous forests, drought responses, early leaf shedding, european heatwaves, land surface phenology, Sentinel-2

Correspondence

Aleixandre Verger, CIDE, CSIC-UV-GV, València 46113, Spain. Tel: (+34) 96 342 41 62; Fax: (+34) 96 342 41 60; Email: verger@csic.es

Editor: Mat Disney

Associate Editor: Gaia Vaglio Laurin

Funding Information

This research was supported by the Spanish Government grant PID2019-110521GB-I00, the Fundación Ramón Areces grant ELEMENTAL-CLIMATE and the Catalan Government grant SGR2017-1005.

Received: 7 April 2022; Revised: 21 June 2022; Accepted: 21 July 2022

doi: 10.1002/rse2.296

Remote Sensing in Ecology and Conservation 2023;9 (1):76–89**Abstract**

Heatwaves and droughts are becoming more common and severe in Europe, causing changes in tree phenology, disrupting the sequestration of carbon and causing tree mortality on a continental scale. The responses of leaf shedding to heatwaves and droughts remain uncertain, although temperate deciduous forests may shed their leaves if exposed to extreme heat and water stress. Little information, however, is available about the extent and recurrence of early leaf shedding induced by drought, likely because it occurs in small forest patches and can be discriminated only during a few weeks. We used highly spatiotemporal Sentinel-2 data as evidence of widespread drought-induced early leaf shedding in Europe during 2017–2021. We estimated the timing of leaf shedding from NDVI time series and a threshold-based method that extracts the end of the growing season. Then, we evaluated the heatwave and drought impacts at the end of season by analysing the z-score of Landsat-7 and -8 land surface temperature and the ERA5-Land air temperature and aridity index. The 10-m resolution Sentinel-2 data identified early leaf shedding not detected by the low-resolution (250 m) MODIS sensor. Early leaf shedding was observed across Europe during the entire study period and its occurrence was linked to preceding anomalously high temperatures and arid conditions. Our results also indicated that mean summer NDVI decreased significantly in the years following early leaf shedding, suggesting a legacy decline in vegetation productivity. Our study demonstrates that decametric satellite data can be used to monitor the responses of forests to extreme climate events at the canopy level and indicates that early leaf shedding associated with heatwaves and droughts is more widespread and frequent across the continent than previously thought.

Introduction

Increases in temperature have lengthened the growing season over the last few decades (Menzel et al., 2006); leaf unfolding has advanced and leaf shedding has delayed in Central Europe. These changes in vegetation phenology have increased the uptake of carbon by vegetation (Keenan et al., 2014). How vegetation phenology will respond to future climatic warming and to extreme climate, however, remains unclear, particularly for leaf shedding, which remains insufficiently studied (Gallinat et al., 2015).

Growing evidence suggests that heatwaves and droughts reduce the sequestration of carbon by vegetation (Bastos et al., 2020; Ciais et al., 2005), and heatwaves such as the European heatwave in 2003 have legacy effects and reduce carbon sequestration in the following years (Ciais et al., 2005). Drought is also an important cause of tree mortality in Europe, and drought is expected to worsen, potentially increasing tree mortality (Hartmann et al., 2022; Senf et al., 2020). Studies on the response of leaf shedding to heatwaves and droughts, however, have provided divergent results, and a deeper understanding of

leaf shedding is needed to forecast atmospheric carbon levels and reduce uncertainties in climatic projections.

One line of research suggests that leaf shedding may be delayed in response to high temperatures in autumn and the presence of heatwaves and droughts. A study in North America using remotely sensed data indicated that drought stress delayed the start of dormancy (Xie et al., 2015). Another study found a positive correlation between the end of the growing season, estimated from satellite data, and a drought index in temperate biomes (Bórnez et al., 2021), and *in situ* measurements indicated that foliar longevity in deciduous trees was greater during the 2003 European heatwave than in previous years (Leuzinger et al., 2005). Manipulative experiments found that heat stress or dry air had no effect on the start of leaf shedding. (Mariën et al., 2021).

Another line of research suggests that the timing of leaf shedding in temperate deciduous forests cannot be delayed further, because photoperiod triggers leaf shedding in autumn (Way & Montgomery, 2015). Leaf shedding may even advance with climatic warming because shedding is linked to increased summer productivity (Zani et al., 2020), which is expected to increase with rising temperatures. Drought-induced early leaf shedding has been reported from local observations, some as far back as the 1913 drought in the United States of America (Kozlowski, 1976). Early leaf shedding in response to heatwaves and droughts, however, has been poorly documented using remotely sensed data, and only one recent study found satellite evidence of early leaf wilting during the 2018 European heatwave (Brun et al., 2020).

Land surface phenology is studied using the seasonality of vegetation observed from remotely sensed observations, and links satellite time series with *in situ* observations of phenophases, near-surface remote sensing and carbon fluxes (Bornez et al., 2020; Bórnez et al., 2020). Literature on land surface phenology studies have focused mainly on moderate- to low-resolution optical satellite data (spatial resolution >100 m), including data from MODIS (Zhang et al., 2003), AVHRR (Julien & Sobrino, 2009) and Proba-V (Bornez et al., 2020), but also other satellite sensors such as the microwave-derived vegetation optical depth (Jones et al., 2011). The spatial resolution of remotely sensed satellite data, however, has an impact on the estimation of phenological metrics (Hmimina et al., 2013), and low resolution may hamper the detection of early leaf shedding; land surface phenology metrics at moderate resolutions generally delay the date of the end of the growing season, particularly in heterogeneous landscapes. The date of early leaf shedding from moderate-resolution satellite data may thus be underestimated or remain undetected when shedding occurs in small forest patches.

The seasonality of vegetation is commonly observed with time series of vegetation indices such as the normalized difference vegetation index (NDVI), enhanced vegetation index (EVI) and the chlorophyll/carotenoid index (CCI) (Yang et al., 2022). Land surface phenology can be also studied using biophysical variables such as leaf area index or gross primary productivity. The study of land surface phenology with vegetation indices can be divided into two broad categories: structural and physiological indices (Yin et al., 2020). Structural indices such as NDVI rely heavily on changes in the near-infrared spectrum and, thus, reflect seasonal changes in leaf biomass. Physiological indices such as CCI are commonly calculated using narrow spectral bands in the visible light spectrum to represent the leaf pigment pool and, thus, are best suited for tracking the photosynthetically active season (Gamon et al., 2016).

The recent launch of decametric-resolution satellites with short revisiting times enables the extraction of land surface phenology metrics at the canopy scale. Sentinel-2 provides images at 10-m resolution. The revisiting time is 5 days at the equator but increases with latitude and can provide daily observations above 65° latitude (Descals et al., 2020). Previous studies have estimated land surface phenology metrics from Sentinel-2 at the canopy level on a continental scale (Bolton et al., 2020; Descals et al., 2020) and have linked land surface phenology metrics with *in situ* observations of phenophases and PhenoCam time series (Tian et al., 2021). Other optical satellite constellations that allow the estimation of land surface phenology metrics include Landsat at the decametric scale (Li et al., 2019) and PlanetScope at the 3-m spatial resolution (Cheng et al., 2020). Land surface phenology metrics in temperate mixed forests can be also estimated using the active C-band sensor in Sentinel-1 (Frison et al., 2018). High-resolution satellite data can potentially improve the monitoring of future responses of forests to climate change and, particularly, to heatwave and droughts (Hartmann et al., 2022). Sentinel-2 may enable the detection of early leaf shedding on a continental scale, quantifying the advance of early leaf shedding and its link to climate extremes.

A recent study explored the feasibility of using 10-m Sentinel-2 data for the detection of early leaf wilting during the 2018 European heatwave (Brun et al., 2020). However, it remains unclear whether 10-meter resolution can be used to monitor early stages of leaf senescence at a broader continental scale, including what the methodological challenges are. Furthermore, it remains unclear whether early leaf wilting and the subsequent leaf shedding are limited to the 2018 European heatwave or more widespread and recurrent across the continent. Finally, to our knowledge, there has never been evidence of a legacy effect of early leaf shedding, nor have legacy effects been studied with a 10-meter resolution. To answer these

questions, we studied the occurrence of early leaf shedding and its link to summer weather conditions in European temperate deciduous forests using Sentinel-2 data for widespread early leaf shedding across Europe during 2017–2021. We quantified the evidence of shifts in the dates of leaf shedding across the continent and compared them to low-resolution phenological data from MODIS. We inspected the legacy effects on the mean NDVI in summer in the years after the early leaf shedding. Finally, we investigated the link between the dates of early leaf shedding and temperature and aridity, to determine whether leaf shedding advances or delays as a response of summer weather conditions.

Materials and Methods

Study area

We investigated the occurrence of early leaf shedding in Europe during 2017–2021. The study area was limited to Europe because it is the only region covered by Sentinel-2 Level 2A for this period, with the rest of the globe only covered during 2019–2021. The study area covered the southern and central distribution of temperate deciduous forests in Europe, between 43 and 55°N and 3°W and 36°E, excluding the north-eastern part of the boundary. This slightly longer coverage allowed a more robust temporal analysis that linked early leaf shedding and summer weather conditions. Europe experienced severe heatwaves and droughts during the Sentinel-2 period (Bastos et al., 2020; Kew et al., 2019; Sánchez-Benítez et al., 2022). The climate of the region is mostly temperate, but the southern part has a Mediterranean climate, where arid conditions in summer are more severe than in Central Europe. This difference in climate accounts for the different composition of tree species in the study area; drought-tolerant deciduous species such as *Quercus faginea* and *Q. frainetto* grow under the Mediterranean climate in southern Europe, and common temperate deciduous species such as *Q. ruber* and *Fagus sylvatica* grow primarily at northern latitudes or highly elevated areas that have less severe arid conditions.

Land surface phenology estimation with Sentinel-2

We processed the Sentinel-2 Level-2A (surface reflectance) time series and estimated the end of the growing season (EoS) in the study area during 2017–2021. EoS was estimated using the threshold-based method proposed by (Descals et al., 2020). The method consists of five steps. (1) Invalid observations were masked using the Scene Classification Layer, which is included in the Sentinel-2

Level-2A product. We also masked observations that were flagged as clouds with a probability >65% in the cloud mask generated with the sentinel2-cloud-detector library of the European Space Agency (ESA). (2) We generated a time series of NDVI, that is the normalized difference between the near-infrared and red bands (bands 8 and 4 in Sentinel-2 respectively). (3) The NDVI time series at a revisiting time of 5 days were linearly interpolated at daily steps. (4) EoS was estimated as the day when NDVI decreased in late summer and autumn, exceeding a dynamic threshold. The threshold was defined as 20% of the annual amplitude plus the annual minimum NDVI value. The 20% threshold represents low NDVI values that ensure the estimation of the leaf-shedding date. Threshold values lower than 20% may lead to inconsistent estimates of EoS because of the noise in the NDVI time series during dormancy. (5) EoS was rejected if the gap between the closest valid observations before and after the EoS date was >15 d. We thereby ensured that only high-confidence estimates from dense Sentinel-2 time series were included in the analysis.

We used NDVI in this study because it is a structural vegetation index that can be used as a proxy for leaf biomass (Yin et al., 2020). The decline in NDVI in autumn is linked to the loss of leaf biomass, while EVI and physiological indices, such as CCI, are linked to photosynthetic phenology and they depict earlier stages of leaf senescence that are linked to pigment degradation (Yang et al., 2022). Thus, the EoS estimated using low threshold values of NDVI is better indicated for detecting the timing of leaf shedding. On the contrary, low threshold values in the EVI or CCI time series depict leaf colouring stages while leaf is still present in the tree.

Detection of early leaf shedding

We identified pixels where early leaf shedding could potentially occur when the EoS estimated using Sentinel-2 NDVI time series was earlier than 1 September (Day of Year (DoY) lower than 244). We used this definition because leaf shedding commonly occurs after this date in European deciduous forests. The same criterion was used in a previous study that detected early leaf wilting in Central Europe (Brun et al., 2020). We masked potential false positives of early leaf shedding in these pixels. First, we removed pixels with vegetation that were affected by wildfires. Areas affected by summer wildfires also presented a decline in the NDVI time series, similar to the decrease in areas affected by early leaf shedding. We masked early-EoS pixels that overlapped with the FIRMS active-fire product (Giglio et al., 2016). The FIRMS product has a 1-km spatial resolution and is based on the MODIS MOD14/MYD14 Fire and Thermal Anomalies product. Second, we masked all

types of vegetation that were not deciduous broadleaf forests (DBFs). The DBF mask was obtained from the Copernicus Global Land Cover Layers (CGLS-LC100 Collection 3) at a resolution of 100 m in 2019 (Buchhorn et al., 2020), which included the class 'deciduous broadleaf closed forest (tree canopy >70%)'. We also used the ESA WorldCover 10-m v100, with the class 'Trees', to mask the remaining non-forest pixels. Finally, we applied a convolutional filter to remove isolated pixels that had early EoS. The convolutional filter consisted of a mode filter in a squared kernel of 3x3-pixel size.

The occurrence of early leaf shedding was validated using a random sampling of pixels. We randomly sampled 300 points where Sentinel-2 potentially detected early leaf shedding during 2017–2021 (EoS date before 1 September). The points were sampled such that the minimum distance between two points was >10 km. The validation was done by visual interpretation of Sentinel-2 images. We visualized RGB true-colour Sentinel-2 images (bands 4, 3 and 2, corresponding to the red, green and blue bands) and labelled the points as early leaf shedding if the RGB image indicated that the forest canopy was brownish.

Since we defined early leaf shedding when EoS <244 (before September 1), we labelled the occurrence of early leaf shedding if the forest canopy had signs of leaf coloration at the end of August (between 20 August and 31 August). In cases where EoS < 244 but Sentinel-2 images were not available at the end of August, we also inspected if leaf coloration was present in the Sentinel-2 images on the first days of September (until 10 September). Early leaves shedding might occur earlier than 20 August but, in that scenario, the event can also be identified at the end of August and beginning of September, since leaves do not reappear until the following year.

If a point was a false positive, we also labelled the cause of the false positive by visual interpretation of Sentinel-2 images. For instance, small fires that remain undetected by FIRMS were detected because forests affected by fires have a distinctive spectral signature and can be visually differentiated from early leaf shedding using true colour Sentinel-2 composites. In the case of forest clear-cuttings, the identification was possible not only because of the distinctive spectral signature but also because of the contextual information in the image. Early leaf shedding occurs in irregularly shaped forest patches, whereas clear-cuttings occur in well-defined shapes corresponding to plantation areas. Lastly, we also checked if the following year in the time series showed any seasonality, and if it did not, we dismissed the point as early leaf shedding. If there is no seasonality in the time series the following year, the occurrence could be tree mortality rather than early leaf shedding.

The Sentinel-2 EoS was compared to the EoS estimated from MODIS. We used the MOD13Q1 version 6, which provides 16-day NDVI time series at 250-m spatial resolution. We estimated the EoS using a dynamic threshold of 20% of the amplitude plus the annual minimum NDVI, as we did with Sentinel-2. The aim of this comparison was to determine whether low resolution (MODIS product at 250-m resolution) could detect early leaf shedding. The data were compared at the points where early leaf shedding was confirmed by visual inspection during 2017–2021. We also investigated whether the size of the forest affected by early leaf shedding influenced the MODIS EoS metrics. We hypothesized that the larger the affected area, the better MODIS EoS could identify early leaf shedding, resulting in a decrease in the difference between the Sentinel-2 EoS and MODIS EoS metrics. To test this hypothesis, we calculated the difference between the two sensors (MODIS EoS – Sentinel-2 EoS). Then, we fitted the difference in EoS as a function of the area affected by early leaf shedding. The affected forest area was calculated as the number of Sentinel-2 10-m pixels that present early leaf shedding (DoY <244) within a 250-m MODIS pixel.

Legacy effects of early leaf shedding

We investigated whether early leaf shedding affected the productivity of the forests in the years after the occurrence by identifying the trends in Sentinel-2 NDVI. We extracted the mean NDVI for early summer (June and July), when NDVI in DBFs peaks during the growing season. We then analysed the trends in NDVI in the pixels early leaf shedding was confirmed by visual interpretation. We inspected whether the NDVI significantly decreased the year after the early leaf shedding. We used a two-sample *t*-test to determine if the mean summer NDVI differed significantly between years with a confidence interval > 95%.

Assessment of heatwave and drought impacts on leaf shedding

The relationship between EoS and extreme climate was investigated using three climatic time series: surface temperature, air temperature and the aridity index. We used the air temperature 2 m above the surface provided by the ERA5-Land hourly dataset (Muñoz-Sabater et al., 2021). The aridity index (P/PET^{-1}) is the ratio of rainfall to potential evapotranspiration for a given time interval (Sherwood & Fu, 2014). The rainfall was obtained directly from the ERA5-Land hourly dataset. Potential evapotranspiration was calculated hourly using the method described by (Singer et al., 2021), which was

based on the FAO Penman–Monteith equation. The spatial resolution of ERA5-Land is 0.1° , which is approximately 9 km. We also used the land surface temperature from Landsat-7 and Landsat-8 (Level 2 Collection 2 Tier 1). The 30-m spatial resolution of Landsat provides images with much greater detail than ERA5-Land, allowing for a more accurate characterization of weather impacts on leaf shedding.

We examined the relationships between temperature, aridity index and the EoS date to identify two types of processes.

1. We investigated whether deciduous trees advanced the leaf shedding date after anomalous high temperatures and arid periods (*i.e.* low values of the aridity index). To do this, we first extracted the mean land surface temperature, mean air temperature and mean aridity before the date of early leaf shedding using various time intervals (15, 30, 60, 90 and 120 days). We then extracted the mean surface temperature, mean air temperature and mean aridity for the same day of the year (DoY) but for other years of the 2001–2021 period. Finally, we tested whether temperature and aridity were significantly different in the year with early leaf shedding and for the other years of 2017–2021 compared to the reference period 2001–2021. The data for temperature and aridity were normalized (z-score) using the reference period 2001–2021, so that the mean was 0 and the standard deviation was 1. Assuming a Gaussian distribution, anomalous temperature and aridity will have a normalized value differing substantially from 0.
2. We investigated whether deciduous trees delay the leaf shedding date when mean summer temperature and aridity are higher. For this case, we estimated the mean air temperature and mean aridity for summer (June, July, August and September) during 2001–2021, the period for which MODIS data were available. We then calculated the sensitivity of the MODIS EoS to mean summer air temperature and mean summer aridity. The sensitivities to air temperature and aridity were calculated as the linear slopes between EoS and the mean air temperature and mean aridity, respectively, using an ordinary least-squares regression over all DBF pixels in the study area. For this analysis, the 250-m MODIS EoS was resized to the spatial resolution of ERA5-Land (9 km).

All geospatial data used in this study were accessed with Google Earth Engine (Gorelick et al., 2017) and processed with this cloud-based platform and Python packages. Moreover, a user interface was developed in Google Earth Engine for the visual interpretation of early leaf shedding in Sentinel-2 images.

Results

Detection of early leaf shedding

We identified 174 points with early leaf shedding from 300 randomly selected locations in pixels where Sentinel-2 EoS was earlier than 1 September (Fig. 1A; Tables S1 and S2). Early leaf shedding was found throughout the study area and study period (2017–2021). Occurrence was highest in 2018 and 2019 (Fig. 1B) and lowest in 2017 and 2021. The insufficient number of valid observations during 2017 was a cause of false positives in our method; a total of 22 points were incorrectly detected as early leaf shedding in 2017, mostly in Central Europe (Fig. 1A). Other causes of false positives were the inaccuracy of the DBF mask (45 points); many locations were in fact shrubland, which may be more prone to early leaf shedding than DBF forests. The early decrease in NDVI was caused by clear-cutting at 27 points and fires at 16 points. Fires were mostly identified in the Apennines and more broadly in the Mediterranean basin, a region that is susceptible to wildfires. We identified these false positives even though the FIRMS active-fire product was used to mask them.

The true-colour Sentinel-2 images revealed the timing before early leaf shedding (Fig. 2A), after early leaf shedding (Fig. 2B) and after all trees had entered dormancy (Fig. 2C) at the 174 points where early leaf shedding was confirmed. The brown colour in the RGB images depicts the areas where trees had coloured leaves or where their leaves were shed. Figure S1 depicts forests that had been cleared or affected by fires, which are disturbances that were also identified visually in Sentinel-2 and discriminated against early leaf shedding.

The Sentinel-2 time series indicated that NDVI for a year with early leaf shedding decreased before 1 September (DoY = 244), substantially earlier than other years during 2017–2021 (Fig. 3). The NDVI time series at two different pixel locations, with early and normal leaf shedding, indicated that the vegetation at both locations had a similar seasonality, with similar EoSs. EoS, however, diverged for the year in which early leaf shedding was detected. The pixels with early leaf shedding had a sharp decrease in NDVI, with subsequent low NDVI values that were similar to those when the deciduous trees became dormant.

The magnitude of the early EoS was underestimated in satellite data with lower spatial resolution. MODIS underestimated the advance in the timing of early leaf shedding (Fig. 4A). Sentinel-2 and MODIS EoS were estimated using a 20% threshold. However, Sentinel-2 generally detected early leaf shedding 40 [18, 65] d (median and

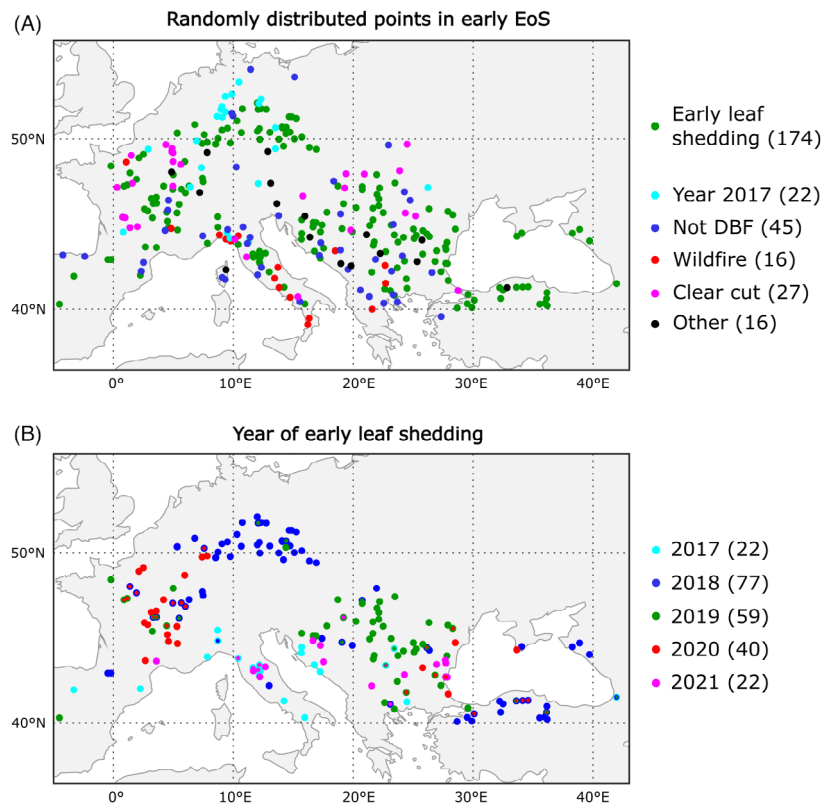


Figure 1. Spatial distribution of the validation points. (A) 300 points were randomly distributed in pixels where the end of the growing season (EoS), obtained with Sentinel-2, was earlier than 1 September. The colours of the points depict the labels assigned during the visual interpretation of Sentinel-2 images. Early leaf shedding was identified in 174 points. False positives appeared in the other points due to the lack of available data in 2017, inaccuracies in the mask for deciduous broadleaf forests (DBFs), the presence of wildfires and clear-cuts and other reasons. (B) The year of detection for the 174 points where early leaf shedding was identified with the visual interpretation of Sentinel-2 images. Early leaf shedding occurred in 220 site-years; some sites experienced early leaf shedding more than once during 2017–2021. The numbers in parentheses represent the number of occurrences.

interquartile range) before MODIS EoS. The differences in EoS between Sentinel-2 and MODIS could be attributed to the use of a different satellite sensors, but the same comparison for the year preceding the early leaf shedding indicated that Sentinel-2 EoS was close to the MODIS EoS (the difference was -15 [-36 , 2] d; Fig. S2), thus indicating that the difference between sensors had a marginal impact on the difference between Sentinel-2 and MODIS EoS.

The difference between the Sentinel-2 and MODIS EoS decreased as the size of the forest affected by early leaf shedding increased (Fig. 4B), indicating that the EoS for both sensors became more similar as the effect grew in size. The slope was significant at a confidence interval of 95%. On average, the difference between Sentinel-2 and MODIS EoS was close to zero when more than 500 Sentinel-2 pixels within a 250-meter MODIS pixel ($>80\%$ of MODIS pixel) presented early leaf shedding.

Legacy effects of early leaf shedding

The overall mean summer NDVI decreased in the year after the early leaf shedding (Fig. 5). The two-sample t -test indicated that the decrease was significant (95% confidence interval) for early leaf shedding that occurred in 2017 and 2018. The decrease was not significant between 2019 and 2020, but the difference was significant compared with the summer NDVI in 2017. These results suggest that summer NDVI decreased not only after the year of early leaf shedding but also in the years preceding it. This negative trend in NDVI was clear when early leaf shedding occurred in 2020 and 2021. The slope of this trend differed significantly from 0 for a confidence interval of 95%. The validity of this analysis, however, was hampered by the short time series; this analysis only included the 5 years of the Sentinel-2 data. Moreover, the NDVI did not decrease the year after early leaf shedding in some of the sites (see site 71 in Fig. 3).

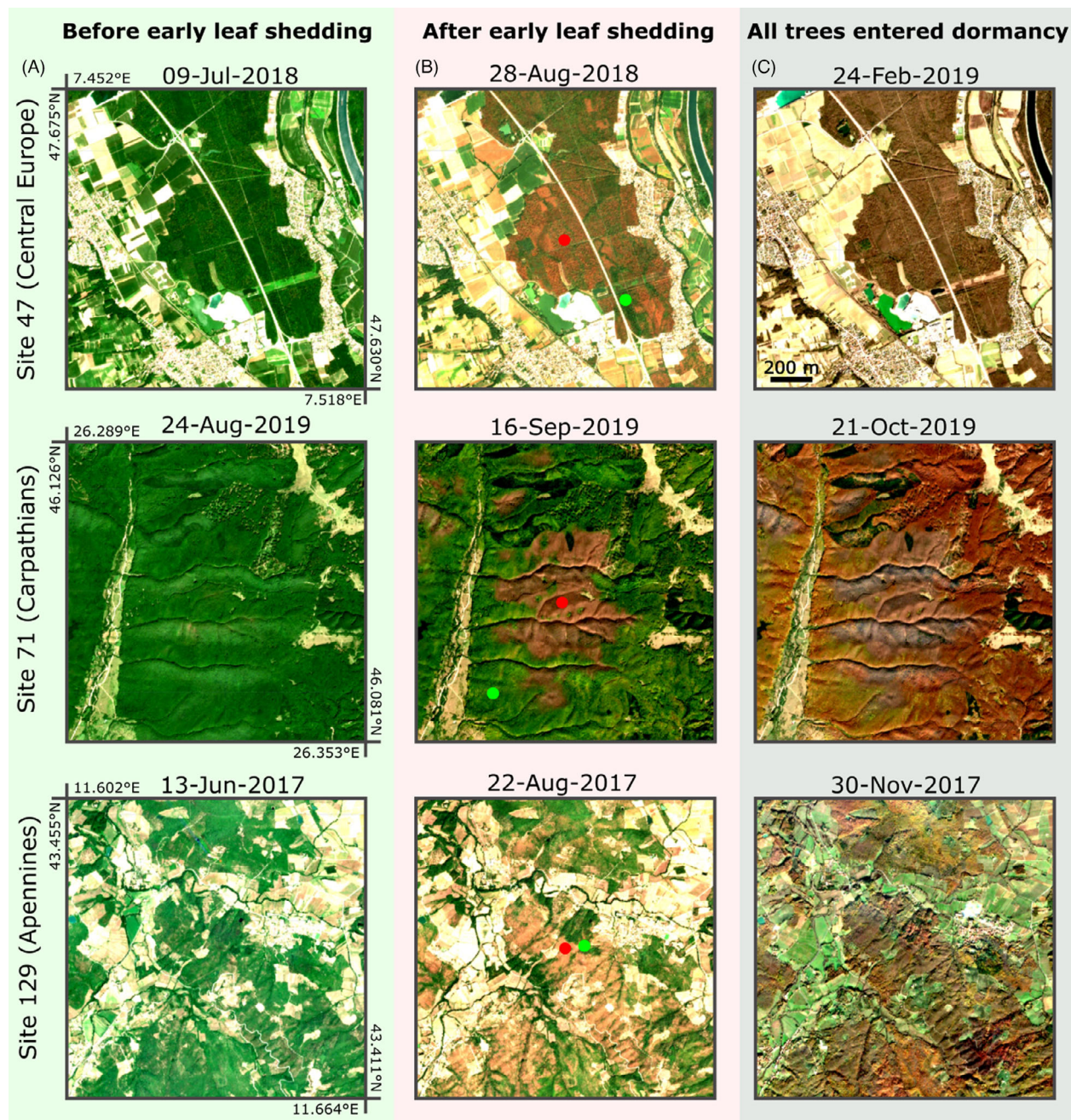


Figure 2. Sentinel-2 images for three sites and three moments of the season: (A) before early leaf shedding, (B) after early leaf shedding and (C) after all trees have entered dormancy. The images show a true-colour composition; the channels correspond to Sentinel-2 bands 4 (red), 3 (green) and 2 (blue). Forests that have shed leaves prematurely in the growing season are depicted by brown in the middle images. The red and green points correspond to pixels whose time series are displayed in Figure 3.

Assessment of heatwaves and drought impacts on leaf shedding

Early leaf shedding generally occurred at anomalously high temperatures and aridity (Fig. 6). The normalized (z-score) land surface temperature, air temperature and

aridity 30 days before early leaf shedding were 0.44 [0.00, 0.98], 0.45 [0.02, 1.31] and -0.64 [-1.03 , -0.28] respectively. The 30-d surface and air temperatures were significantly higher and the 30-day aridity was significantly lower than the average reference period 2001–2021 for the same DoYs ($P < 0.05$). When considering other

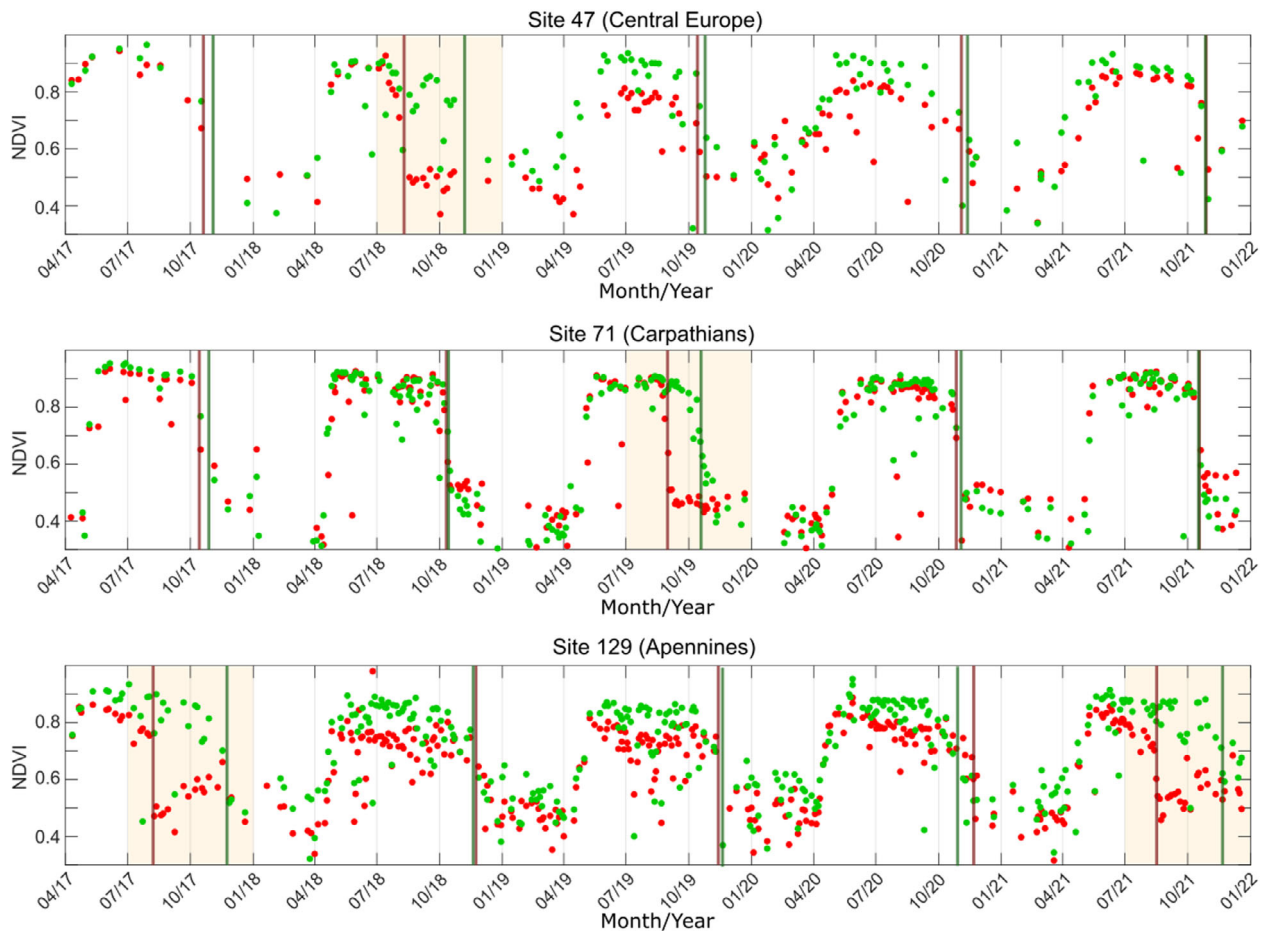


Figure 3. Time series of the normalized difference vegetation index (NDVI) for a canopy with early leaf shedding (red points) and a canopy that shed its leaves near the median of 2017–2021 (green points) at three sites (Figure 2). The time of the year when early leaf shedding was detected is indicated by the beige shading. The site locations are shown in Figure 2.

aggregation periods (15, 60, 90 and 120 days before early leaf shedding), the mean temperature and mean aridity were also significantly different from the long-term averages (Fig. S3).

The analysis above considered aggregated mean temperature and aridity for all the sites where early leaf shedding was detected. The period under which weather conditions affect early leaf shedding, however, may differ locally. The area of early leaf shedding increased for specific years when conditions were driest (Fig. 7), corroborating the finding in Fig. 6, but the length of time under which the conditions were arid depended on the region. For example, a short period of arid conditions led to leaf shedding in the Carpathians (Fig. 7b), while forests shed their leaves after a longer arid period in the Apennines and Central Europe (Fig. 7A and C).

The sensitivity of MODIS EoS was positive ($0.60 \text{ d } ^\circ\text{C}^{-1}$) to summer mean air temperature and negative ($-1.76 \text{ d mm mm}^{-1}$) to summer mean aridity during

2001–2021, indicating that EoS was delayed with hotter and drier summers. However, the percentage of pixels with significant sensitivity was relatively low; 5.27 and 4.78% of the pixels covering DBFs had a significant sensitivity of EoS to temperature and aridity respectively (Fig. 8).

Discussion

Sentinel-2 was able to identify early leaf shedding at the continental scale during 2017–2021. Early leaf shedding occurred not only during extreme short-term heatwaves, such as the 2018 European heatwave, but in every year during 2017–2021 when weather conditions were less severe. The estimation of early EoS was possible due to the short revisiting times of the Sentinel-2A and -2B satellites. The MODIS EoS product greatly underestimated early leaf shedding. Low spatial resolution tends to overestimate the length of the growing season (Hmimina et al., 2013), which hampers the retrospective study of

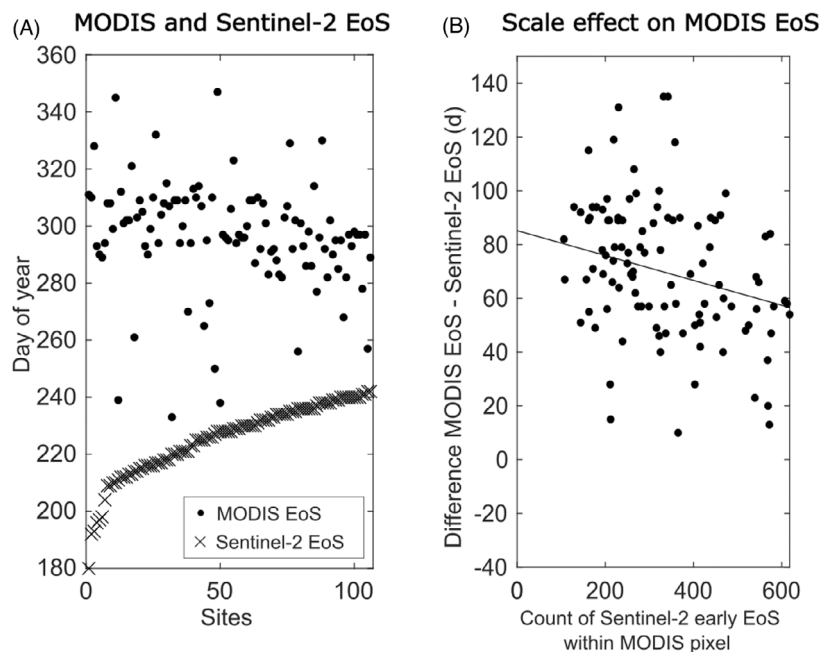


Figure 4. Comparison between the end of the growing season (EoS) obtained from MODIS and Sentinel-2 for 174 sites where early leaf shedding was detected. (A) Representation of the Sentinel-2 EoS and the MODIS EoS metrics per site. The EoS metrics were estimated with a 20% threshold using the Sentinel-2 and MODIS NDVI time series. Sites are numbered with the Sentinel-2 EoS in ascending order. We show only 106 sites, which are the sites where the MODIS EoS metrics were available. (B) Effect of scale on the estimates of early leaf shedding in MODIS. The x-axis shows the number of pixels in which Sentinel-2 detected early leaf shedding within a 250-m MODIS pixel. The y-axis shows the difference between the Sentinel-2 EoS and the MODIS EoS metrics at each site.

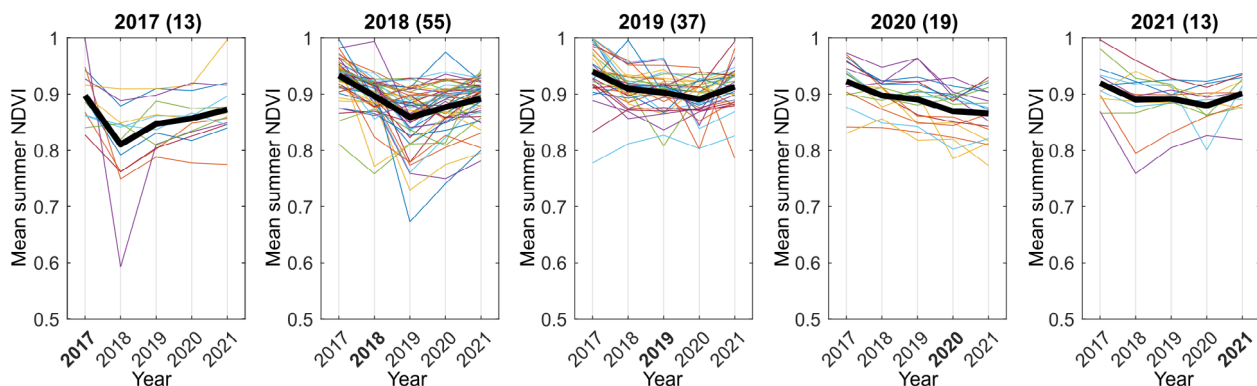


Figure 5. Mean summer normalized difference vegetation index (NDVI) at sites where early leaf shedding was observed during 2017–2021. The sites were grouped depending on the year of the occurrence. The titles show the year of disturbance and the number of sites in parentheses. Only sites with 1 year of early leaf shedding during 2017–2021 were considered. The thin lines represent the summer NDVI per site and the thick line represents the mean summer NDVI across sites.

early leaf shedding before the era of Sentinel-2 or Landsat-7 and -8. The bias between Sentinel-2 and MODIS differed greatly among sites. Our results indicated that these differences depended on the varying sizes of the areas that experienced early leaf shedding. MODIS may thus detect early leaf shedding more accurately when it occurs in large areas, reducing the bias associated with

the Sentinel-2 estimate. Early leaf shedding in European temperate deciduous forests, however, occurs mainly at a small scale and can be observed only during the last weeks of the growing season in late summer and early autumn. In contrast, tree mortality in coniferous trees can be easily detected with decametric-resolution satellite images in the following growing season (Meddens

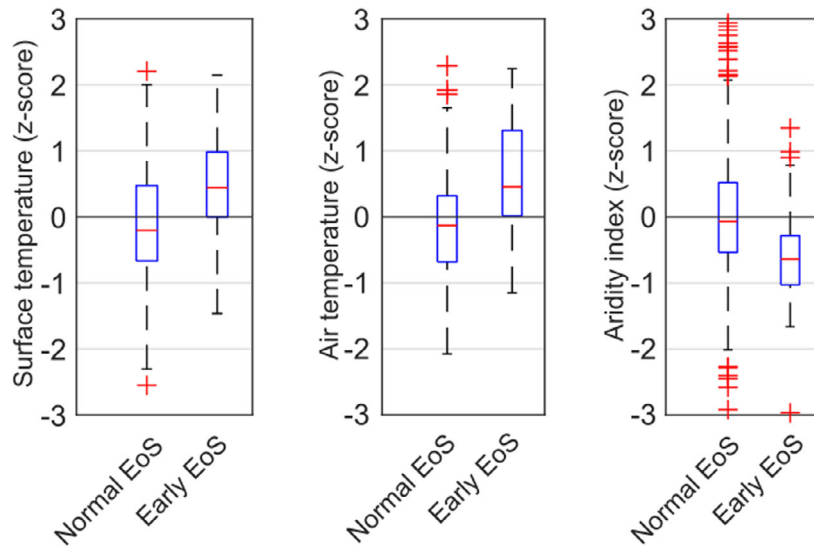


Figure 6. Anomalies of land surface temperature, air temperature and aridity (P_{PET}^{-1}) at the 174 sites where early leaf shedding was identified. Land surface temperature, air temperature and aridity were calculated for a time lag of 30 d before early leaf shedding. The boxplots depict the temperature and aridity distributions normalized (z-score) using the reference period 2001–2021. 'Early EoS' represents the year of early leaf shedding detected during 2017–2021, and 'normal EoS' represents other years during 2017–2021. Red line depicts the median, blue box represents the interquartile range and red crosses outside the whiskers are outliers (>2 and <-2 standard deviations).

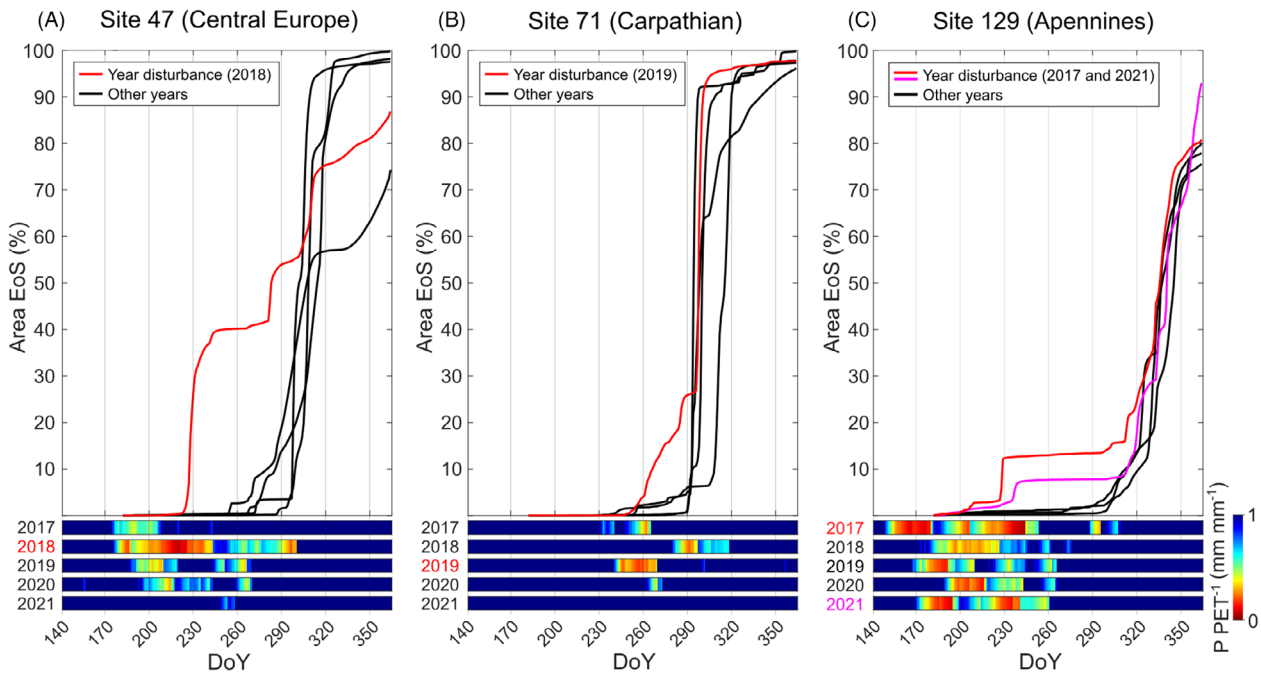


Figure 7. Accumulated area that reached the end of the growing season (EoS) at three sites in (A) Central Europe, (B) the Carpathians, and (C) the Apennines. The accumulated EoS was calculated for an area of $10 \times 10\ km^2$ at each site. Red and magenta lines correspond to years in which early leaf shedding was detected. Black lines are other years during 2017–2021. The lower panels show the 30-d aridity (P_{PET}^{-1}) during 2017–2021.

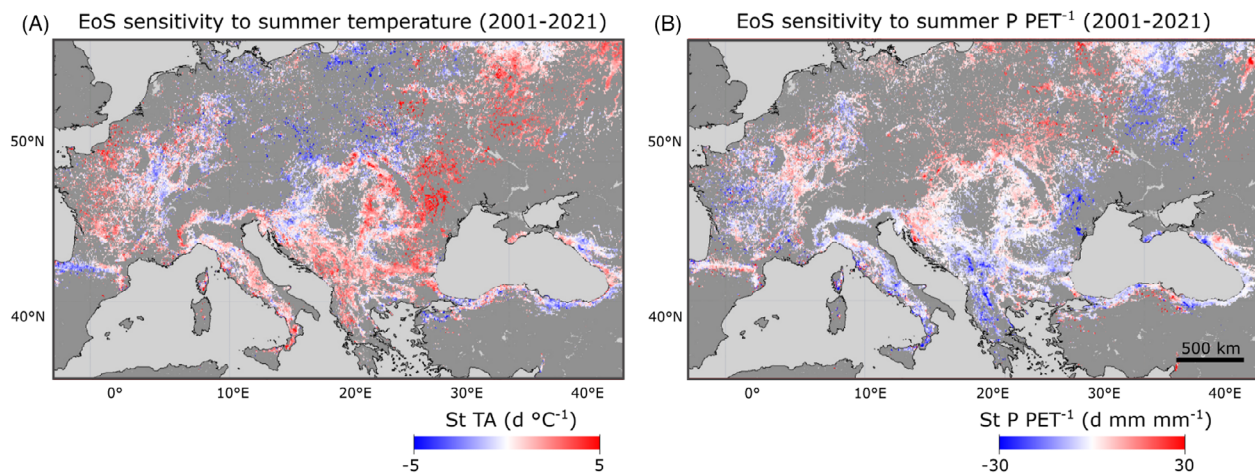


Figure 8. Sensitivity (St) of the end of the growing season (EoS) to (A) mean summer air temperature (TA) and (B) mean summer aridity (P PET⁻¹) during 2001–2021. EoS was estimated using a dynamic threshold of 20% and NDVI time series from the MOD13Q1 product. The maps show only pixels that are classified as deciduous broadleaved forests in the CGLS-LC100 product.

et al., 2013), which may account for why early stages of leaf senescence in DBFs have been insufficiently studied in remote-sensing studies, with only one study using Sentinel-2 data to cover this event (Brun et al., 2020).

Early leaf shedding was linked to unusually high temperatures and aridity in the days preceding the event. Most occurrences were in Central Europe in 2018 and the Carpathians in 2019. These occurrences coincided in time and space with European heatwaves. The data from some sites also suggested that early leaf shedding stopped when aridity decreased (Fig. 7), presumably because rain resumed. Our results indicated a link between early leaf shedding and arid conditions in summer, but the direct causes that trigger leaf shedding remain unknown. Deciduous broadleaved trees may simply shed their leaves to prevent excessive evapotranspiration (Bréda et al., 2006), which may help prevent the stems from desiccating, reducing the likelihood of death. This strategy does not apply to coniferous trees, where hydraulic failure occurs during arid conditions, leading to tree death (Arend et al., 2021). Pest infestations are another plausible cause of early leaf shedding. A previous study found that deciduous trees shed their leaves as a mechanism to control pest populations (Karban, 2007).

Satellite data identified a divergent response of EoS to heatwaves and drought in deciduous forests. The Sentinel-2 data indicated that leaves were shed prematurely in forest patches during the growing season, but the MODIS data indicated that deciduous forests generally delayed leaf shedding during warm and arid seasons. Similar results to MODIS were found with another satellite product at low spatial resolution (Bórnez et al., 2021) and *in situ* observations (Leuzinger et al., 2005). Delayed shedding in an arid

summer may involve a mechanism distinct from early leaf shedding. Heatwaves may induce early leaf shedding locally due to their brief duration but high severity of heat stress. In contrast, continual arid conditions during the summer can reduce vegetation productivity (Ciais et al., 2005), which in turn could account for the delay in leaf shedding (Zani et al., 2020). Such persisting arid conditions throughout the growing season are not severe enough to cause early leaf shedding, which also suggests that early leaf shedding occurs when specific thresholds for heat and water stress are exceeded, but additional evidence is required to support this hypothesis.

Our results indicated that NDVI decreased the year after the early leaf shedding, indicating a legacy effect on carbon uptake in the following years. A previous study found that carbon sequestration decreased after the 2003 European heatwave (Ciais et al., 2005). The effect of early leaf shedding on the annual carbon uptake nevertheless remains uncertain. Annual carbon uptake may not be affected, because carbon uptake in spring increases due to early SoS and high spring temperatures (Bastos et al., 2020). Our findings indicate that future increases in heatwave and drought events will negatively influence carbon uptake in temperate forests. More extreme droughts will lead to forests shedding their leaves prematurely, as we have demonstrated. These forests will cease to take up carbon very early in the growing season.

Our method is based on the estimation of the EoS date. We used low threshold values of NDVI to ensure the detection of leaf shedding, but it is not entirely clear whether the decrease in NDVI was due to actual leaf shedding or simply wilting. More validation exercises using *in situ* observations of leaf phenophases are needed

to confirm whether the NDVI-based EoS from Sentinel-2 represents leaf shedding. Moreover, we also found shortcomings in our method that hampered the estimation of EoS using the Sentinel-2 data. One shortcoming was the low availability of data in cloud-prone regions. The frequency of observations could be increased by including data from Landsat satellites, which would improve the confidence of EoS estimates, particularly in 2017 when only images from Sentinel-2A were available and the revisit time was 10 days. Our method of detection could be improved with more accurate forest masks and optimized algorithms for detecting clouds, as (Brun et al., 2020) have done for Central Europe. These improvements would reduce false positives, allowing for confident estimates of areas of early leaf shedding following the practices used by (Olofsson et al., 2014). Additionally, our method would also benefit from a burned area product based on Sentinel-2 data at a decametric resolution. The FIRMS active fire product was unable to filter small fires and, thus, our method detected these burned areas because these areas showed a drop in NDVI, which is also typical of early leaf shedding. Lastly, we found false positives associated with clear-cutting. These false positives are more difficult to detect automatically, and future algorithms for monitoring early leaf shedding should take this difficulty into account, particularly for Central Europe where this harvesting practice is common.

Our study demonstrates the feasibility of using decametric satellite data to monitor forest responses to drought at the canopy level. Sentinel-2 acquisitions are freely delivered in near real-time with a resolution of 10 m, enabling the rapid detection and localization of early leaf shedding. Our method may thus facilitate *in situ* observations by helping define the area to visit when an event occurs. These local observations would contribute to a better understanding of the factors that contribute to early leaf shedding. The causes of early leaf shedding are difficult to deduce from satellite data alone, and field observations are required to confirm the underlying mechanisms. Future research may also examine the decrease in NDVI in the years preceding early leaf shedding, which could be attributed to the effects of global warming on forest health in Europe.

Acknowledgements

This work represents a contribution to CSIC Thematic Interdisciplinary Platform TELEDTECT.

This research was supported by the Spanish Government grant PID2019-110521GB-I00, the Fundación Ramón Areces grant ELEMENTAL-CLIMATE and the Catalan Government grant SGR2017-1005.

References

- Arend, M., Link, R.M., Patthey, R., Hoch, G., Schuldt, B. & Kahmen, A. (2021) Rapid hydraulic collapse as cause of drought-induced mortality in conifers. *Proceedings of the National Academy of Sciences of the United States of America*, **118**(16), e2025251118.
- Bastos, A., Ciais, P., Friedlingstein, P., Sitch, S., Pongratz, J., Fan, L. et al. (2020) Direct and seasonal legacy effects of the 2018 heat wave and drought on European ecosystem productivity. *Science Advances*, **6**(24), eaba2724.
- Bolton, D.K., Gray, J.M., Melaas, E.K., Moon, M., Eklundh, L. & Friedl, M.A. (2020) Continental-scale land surface phenology from harmonized Landsat 8 and Sentinel-2 imagery. *Remote Sensing of Environment*, **240**, 111685.
- Bórnez, K., Richardson, A.D., Verger, A., Descals, A. & Peñuelas, J. (2020) Evaluation of vegetation and proba-v phenology using phenocam and eddy covariance data. *Remote Sensing*, **12**(18), 3077.
- Bórnez, K., Descals, A., Verger, A. & Peñuelas, J. (2020) Land surface phenology from VEGETATION and PROBA-V data. Assessment over deciduous forests. *International Journal of Applied Earth Observation and Geoinformation*, **84**, 101974.
- Bórnez, K., Verger, A., Descals, A. & Peñuelas, J. (2021) Monitoring the responses of deciduous Forest phenology to 2000–2018 climatic anomalies in the northern hemisphere. *Remote Sensing*, **13**(14), 2806.
- Bréda, N., Huc, R., Granier, A. & Dreyer, E. (2006) Temperate forest trees and stands under severe drought: a review of ecophysiological responses, adaptation processes and long-term consequences. *Annals of Forest Science*, **63**(6), 625–644.
- Brun, P., Psomas, A., Ginzler, C., Thuiller, W., Zappa, M. & Zimmermann, N.E. (2020) Large-scale early-wilting response of central European forests to the 2018 extreme drought. *Global Change Biology*, **26**(12), 7021–7035.
- Buchhorn, M., Lesiv, M., Tsendbazar, N.E., Herold, M., Bertels, L. & Smets, B. (2020) Copernicus global land cover layers—collection 2. *Remote Sensing*, **12**(6), 1044.
- Cheng, Y., Vrieling, A., Fava, F., Meroni, M., Marshall, M. & Gachoki, S. (2020) Phenology of short vegetation cycles in a Kenyan rangeland from PlanetScope and Sentinel-2. *Remote Sensing of Environment*, **248**, 112004.
- Ciais, P., Reichstein, M., Viovy, N., Granier, A., Ogée, J., Allard, V. et al. (2005) Europe-wide reduction in primary productivity caused by the heat and drought in 2003. *Nature*, **437**(7058), 529–533.
- Descals, A., Verger, A., Yin, G. & Peñuelas, J. (2020) Improved estimates of arctic land surface phenology using Sentinel-2 time series. *Remote Sensing*, **12**(22), 3738.
- Frison, P.-L., Fruneau, B., Kmiha, S., Soudani, K., Dufrêne, E., Toan, T.L. et al. (2018) Potential of Sentinel-1 data for monitoring temperate mixed forest phenology. *Remote Sensing*, **10**(12), 2049.

- Gallinat, A.S., Primack, R.B. & Wagner, D.L. (2015) Autumn, the neglected season in climate change research. *Trends in Ecology and Evolution*, **30**(3), 169–176.
- Gamon, J.A., Huemmrich, K.F., Wong, C.Y.S., Ensminger, I., Garrity, S., Hollinger, D.Y. et al. (2016) A remotely sensed pigment index reveals photosynthetic phenology in evergreen conifers. *Proceedings of the National Academy of Sciences of the United States of America*, **113**(46), 13087–13092.
- Giglio, L., Schroeder, W. & Justice, C.O. (2016) The collection 6 MODIS active fire detection algorithm and fire products. *Remote Sensing of Environment*, **178**, 31–41.
- Gorelick, N., Hancher, M., Dixon, M., Ilyushchenko, S., Thau, D. & Moore, R. (2017) Google earth engine: planetary-scale geospatial analysis for everyone. *Remote Sensing of Environment*, **202**, 18–27.
- Hartmann, H., Bastos, A., das, A.J., Esquivel-Muelbert, A., Hammond, W.M., Martínez-Vilalta, J. et al. (2022) Climate change risks to global Forest health: emergence of unexpected events of elevated tree mortality worldwide. *Annual Review of Plant Biology*, **73**, 673–702.
- Himmling, G., Dufrêne, E., Pontailier, J.Y., Delpierre, N., Aubinet, M., Caquet, B. et al. (2013) Evaluation of the potential of MODIS satellite data to predict vegetation phenology in different biomes: an investigation using ground-based NDVI measurements. *Remote Sensing of Environment*, **132**, 145–158.
- Jones, M.O., Jones, L.A., Kimball, J.S. & McDonald, K.C. (2011) Satellite passive microwave remote sensing for monitoring global land surface phenology. *Remote Sensing of Environment*, **115**(4), 1102–1114.
- Julien, Y. & Sobrino, J. (2009) Global land surface phenology trends from GIMMS database. *International Journal of Remote Sensing*, **30**(13), 3495–3513.
- Karban, R. (2007) Deciduous leaf drop reduces insect herbivory. *Oecologia*, **153**(1), 81–88.
- Keenan, T.F., Gray, J., Friedl, M.A., Toomey, M., Bohrer, G., Hollinger, D.Y. et al. (2014) Net carbon uptake has increased through warming-induced changes in temperate forest phenology. *Nature Climate Change*, **4**(7), 598–604.
- Kew, S.f., Philip, S.Y., Jan van Oldenborgh, G., van der Schrier, G., FEL, O. & Vautard, R. (2019) The exceptional summer heat wave in southern Europe 2017. *Bulletin of the American Meteorological Society*, **100**(1), S49–S53.
- Kozłowski, T. (1976) Water supply and leaf shedding. *Soil water measurements, plant responses, and breeding for drought resistance*, **4**, 191–231.
- Leuzinger, S., Zotz, G., Aschhoff, R. & Korner, C. (2005) Responses of deciduous forest trees to severe drought in Central Europe. *Tree Physiology*, **25**(6), 641–650.
- Li, X., Zhou, Y., Meng, L., Asrar, G.R., Lu, C. & Wu, Q. (2019) A dataset of 30 m annual vegetation phenology indicators (1985–2015) in urban areas of the conterminous United States. *Earth System Science Data*, **11**(2), 881–894.
- Mariën, B., Dox, I., de Boeck, H.J., Willems, P., Leys, S., Papadimitriou, D. et al. (2021) Does drought advance the onset of autumn leaf senescence in temperate deciduous forest trees? *Biogeosciences*, **18**(11), 3309–3330.
- Meddens, A.J., Hicke, J.A., Vierling, L.A. & Hudak, A.T. (2013) Evaluating methods to detect bark beetle-caused tree mortality using single-date and multi-date Landsat imagery. *Remote Sensing of Environment*, **132**, 49–58.
- Menzel, A., Sparks, T.H., Estrella, N. & Roy, D.B. (2006) Altered geographic and temporal variability in phenology in response to climate change. *Global Ecology and Biogeography*, **15**(5), 498–504.
- Muñoz-Sabater, J., Dutra, E., Agustí-Panareda, A., Albergel, C., Arduini, G., Balsamo, G. et al. (2021) ERA5-land: a state-of-the-art global reanalysis dataset for land applications. *Earth System Science Data Discussions*, **13**(9), 4349–4383.
- Olofsson, P., Foody, G.M., Herold, M., Stehman, S.V., Woodcock, C.E. & Wulder, M.A. (2014) Good practices for estimating area and assessing accuracy of land change. *Remote Sensing of Environment*, **148**, 42–57.
- Sánchez-Benítez, A., Goessling, H., Pithan, F., Semmler, T. & Jung, T. (2022) The July 2019 European heat wave in a warmer climate: storyline scenarios with a coupled model using spectral nudging. *Journal of Climate*, **35**(8), 2373–2390.
- Senf, C., Buras, A., Zang, C.S., Rammig, A. & Seidl, R. (2020) Excess forest mortality is consistently linked to drought across Europe. *Nature Communications*, **11**(1), 1–8.
- Sherwood, S. & Fu, Q. (2014) A drier future? *Science*, **343**(6172), 737–739.
- Singer, M.B., Asfaw, D.T., Rosolem, R., Cuthbert, M.O., Miralles, D.G., MacLeod, D. et al. (2021) Hourly potential evapotranspiration at 0.1° resolution for the global land surface from 1981-present. *Scientific Data*, **8**(1), 1–13.
- Tian, F., Cai, Z., Jin, H., Hufkens, K., Scheffinger, H., Tagesson, T. et al. (2021) Calibrating vegetation phenology from Sentinel-2 using eddy covariance, PhenoCam, and PEP725 networks across Europe. *Remote Sensing of Environment*, **260**, 112456.
- Way, D.A. & Montgomery, R.A. (2015) Photoperiod constraints on tree phenology, performance and migration in a warming world. *Plant, Cell & Environment*, **38**(9), 1725–1736.
- Xie, Y., Wang, X. & Silander, J.A. (2015) Deciduous forest responses to temperature, precipitation, and drought imply complex climate change impacts. *Proceedings of the National Academy of Sciences of the United States of America*, **112**(44), 13585–13590.
- Yang, Y., Chen, R., Yin, G., Wang, C., Liu, G., Verger, A. et al. (2022) Divergent performances of vegetation indices in extracting photosynthetic phenology for northern deciduous broadleaf forests. *IEEE Geoscience and Remote Sensing Letters [Preprint]*, **19**, 1–5.

- Yin, G., Verger, A., Filella, I., Descals, A. & Peñuelas, J. (2020) Divergent estimates of forest photosynthetic phenology using structural and physiological vegetation indices. *Geophysical Research Letters*, **47**(18), e2020GL089167.
- Zani, D., Crowther, T.W., Mo, L., Renner, S.S. & Zohner, C.M. (2020) Increased growing-season productivity drives earlier autumn leaf senescence in temperate trees. *Science*, **370**(6520), 1066–1071.
- Zhang, X., Friedl, M.A., Schaaf, C.B., Strahler, A.H., Hodges, J.C.F., Gao, F. et al. (2003) Monitoring vegetation phenology using MODIS. *Remote Sensing of Environment*, **84**(3), 471–475.

Supporting Information

Additional supporting information may be found online in the Supporting Information section at the end of the article.

Table S1. List of the 174 randomly distributed points where early leaf shedding was detected with Sentinel-2 for 2017–2021.

Table S2. List of the 126 randomly distributed points where false positives of early leaf shedding were detected with Sentinel-2 for 2017–2021. The column ‘Comment’ categorises the cause of the false positives; low availability

of data in 2017 (2017), presence of clear-cutting (‘Clear-cut’), land cover is not deciduous broadleaved forest (Not DBF), presence of wildfires (Wildfire), and other reasons (Other).

Figure S1. Six validation points where Sentinel-2 detected an early end of the growing season (before 1 September). The upper images show a true-colour Sentinel-2 composition of clear-cutting, and the lower images show forests that were affected by wildfires.

Figure S2. Comparison between the end of the growing season (EoS) obtained from MODIS and Sentinel-2 for 174 sites. The comparison was for the year before premature leaf shedding was detected. Sites are numbered with the Sentinel-2 EoS in ascending order. We show only 92 sites, which are the sites where the MODIS EoS metrics were available.

Figure S3. Anomalies of land surface temperature, air temperature and aridity ($P \text{ PET}^{-1}$) at the 174 sites where early leaf shedding was identified. Temperature and aridity were calculated for four intervals: 15, 60, 90, and 120 days before early leaf shedding. The boxplots depict the distributions of temperature and aridity normalised (z-score) using the reference period 2001–2021. ‘Early EoS’ represents the year of early leaf shedding detected during 2017–2021, and ‘normal EoS’ represents other years during 2017–2021.